Amino Acids (2007) 33: 113–121
DOI 10.1007/s00726-006-0412-0
Printed in The Netherlands

Amino Acids

# Multi-layered network structure of amino acid (AA) metabolism characterized by each essential AA-deficient condition

**N. Shikata**[1], **Y. Maki**[2], **Y. Noguchi**[3], **M. Mori**[3], **T. Hanai**[1], **M. Takahashi**[3], and **M. Okamoto**[1]

[1] Graduate School of Systems Life Sciences, Kyushu University, Fukuoka, Japan
[2] Department of Digital Media, Fukuoka International University, Fukuoka, Japan
[3] Research Institute for Health Fundamentals, Ajinomoto Co., Inc., Kawasaki, Japan

Received August 4, 2006
Accepted August 28, 2006
Published online October 13, 2006; 

**Summary.** The concentrations of free amino acids in plasma change coordinately and their profiles show distinctive features in various physiological conditions; however, their behavior can not always be explained by the conventional flow-based metabolic pathway network. In this study, we have revealed the interrelatedness of the plasma amino acids and inferred their network structure with threshold-test analysis and multilevel-digraph analysis methods using the plasma samples of rats which are fed diet deficient in single essential amino acid.

In the inferred network, we could draw some interesting interrelations between plasma amino acids as follows: 1) Lysine is located at the top control level and has effects on almost all of the other plasma amino acids. 2) Threonine plays a role in a hub in the network, which has direct links to the most number of other amino acids. 3) Threonine and methionine are interrelated to each other and form a loop structure.

**Keywords:** Plasma amino acids – Profile – Relation – Network – Threonine – Amino acid deficiency

## Introduction

The recent advances in experimental technology made it possible to analyze various kinds of metabolites in biological samples comprehensively. The amounts of the metabolites in biological fluids and tissues change temporally in coordination with physiological conditions in complex metabolic and signaling pathways. Multivariate analysis and pattern recognition studies have revealed that these metabolite profiles contain the phenotypic information which can be used as a signature for a physiological condition (Nicholson et al., 1999).

Amino acids are a group of metabolites which are important as substrates for protein synthesis as well as signaling molecules (Felig, 1975). The plasma amino acid concentrations, like other metabolites, have distinctive features for various physiological conditions. Some diseases such as liver failure (Holm et al., 1999), renal failure (Hong et al., 1998), cancer (Watanabe et al., 1984), diabetes (Watanabe et al., 1983), muscle dysfunction (Jimenez Jimenez et al., 1991) and aminoacidemia (Tudor et al., 1976) have been reported to have specific abnormalities in plasma amino acid profiles. There are some studies which make use of plasma amino acid profiles to diagnosis and distinguish abnormal subjects from healthy subjects, or subtypes and stages of diseases (Noguchi et al., 2006). One of the traditional examples of using plasma amino acid profiles for diagnostic markers is the Fisher's ratio, which is a ratio of branched-chain amino acids to aromatic amino acids and is used for the marker of liver fibrosis (Ferenci and Wewalka, 1978; Soeters and Fischer, 1976). These studies clearly show that plasma amino acid profile itself can be a useful tool for monitoring the physiological state of an organism.

Although these previous studies discuss how to distinguish different physiological states using the plasma amino acid profile data, the control mechanism behind the change in the profile is not thoroughly discussed. Further investigations on the control mechanism of plasma amino acids should uncover the trigger reasons for diseases or propose a new treatment to improve the physiological conditions, however, the control mechanism is so complicated that the investigations have not been succeeded. The reasons for this complexity should come from the interrelatedness of the amino acids and a number of internal and external factors affecting their concentrations. Amino acids are directly and

indirectly related to each other within a large metabolic pathway and their concentrations in the plasma are equivalent to the whole sum of the metabolic flow in each organs and tissues. The metabolic flow in organs and tissues are affected by various factors such as nutrition, diseases, exercise, and body composition, and so does the plasma amino acid profile. Also, there are still unknown metabolic pathways, which are being discovered not only experimentally but also with using automated methods (Chou et al., 2006). From these reasons, the changes in the concentrations of plasma amino acids can not be simply explained by the topological network structure of metabolic pathway map.

In the previous study, we have introduced the correlation based network analysis of plasma and tissue amino acids (Noguchi et al., 2006) and demonstrated the similarity of the behavior of two amino acids in plasma and tissues. In this study, we carried out the network analysis one step further and introduced the directional relationship between plasma amino acids. For this purpose, we used plasma amino acid profile data of rats fed on a single amino acid-deficient (minus-one) diet. In this experimental model, the plasma concentration of deficient amino acid decreases drastically, which also affects the concentration of other amino acids. This resembles the changes observed in the gene expression profile of single gene knock-out models (Yeang et al., 2005). Taking advantage of this resemblance, the methods used for inferring gene expression network structure are adopted in this study for inferring the interrelated and directional network structure of plasma amino acids without considering any prior topological information on metabolic pathways. This data driven analysis should lead us to the further understanding of the dynamics of the plasma amino acid profiles and gives us some clues for the factors affecting the interrelated network under various physiological conditions.

## Materials and methods

*Animals, experimental design and sample collection*

Adult male Sprague-Dawley rats were maintained on a 12:12-h light–dark cycle, with water provided freely. Starting from 10 weeks of age, the rats were randomly assigned and switched to control or one of the experimental diets (n = 6 each). The composition of the diet is based on AIN93G standard diet, slightly modified by replacing dextrin and sucrose by corn starch, and casein by amino acid mixture shown in Table 1. Each experimental diet (minus-one diet) is completely depleted of single essential amino acids; histidine, isoleucine, leucine, lysine, methionine, phenylalanine, threonine, tryptophan and valine. The rats fed branched-chain amino acid (BCAA) minus-one diets were kept for 5 weeks, and those fed other essential amino acid (EAA) minus-one diets were kept for 15 weeks under *ad libitum* feeding condition. Rats were sacrificed 3 h after feeding and blood samples were collected from postcaval vein and mixed with EDTA immediately to prevent coagulation. The plasma separated from the blood samples are mixed with 2 volumes of 5% (w/w) trichloroacetic acid, and centrifuged immediately at 4 °C, 8000 × *g* for 20 minutes. The supernatant

**Table 1.** Amino acid composition in minus-one diet

| %, w/w | Control | −His | −Ile | −Leu | −Lys | −Met | −Phe | −Thr | −Trp | −Val |
|---|---|---|---|---|---|---|---|---|---|---|
| His | 2.54 | 0.00 | 2.54 | 2.54 | 2.54 | 2.54 | 2.54 | 2.54 | 2.54 | 2.54 |
| Ile | 4.45 | 4.45 | 0.00 | 4.45 | 4.45 | 4.45 | 4.45 | 4.45 | 4.45 | 4.45 |
| Leu | 8.13 | 8.13 | 8.13 | 0.00 | 8.13 | 8.13 | 8.13 | 8.13 | 8.13 | 8.13 |
| Lys · HCl | 8.82 | 8.82 | 8.82 | 8.82 | 0.00 | 8.82 | 8.82 | 8.82 | 8.82 | 8.82 |
| Met | 2.43 | 2.43 | 2.43 | 2.43 | 2.43 | 0.00 | 2.43 | 2.43 | 2.43 | 2.43 |
| Phe | 4.50 | 4.50 | 4.50 | 4.50 | 4.50 | 4.50 | 0.00 | 4.50 | 4.50 | 4.50 |
| Thr | 3.81 | 3.81 | 3.81 | 3.81 | 3.81 | 3.81 | 3.81 | 0.00 | 3.81 | 3.81 |
| Trp | 1.08 | 1.08 | 1.08 | 1.08 | 1.08 | 1.08 | 1.08 | 1.08 | 0.00 | 1.08 |
| Val | 5.73 | 5.73 | 5.73 | 5.73 | 5.73 | 5.73 | 5.73 | 5.73 | 5.73 | 0.00 |
| Ah | 2.55 | 2.55 | 2.55 | 2.55 | 2.55 | 2.55 | 2.55 | 2.55 | 2.55 | 2.55 |
| Arg | 3.28 | 3.28 | 3.28 | 3.28 | 3.28 | 3.28 | 3.28 | 3.28 | 3.28 | 3.28 |
| Asn · $H_2O$ | 3.60 | 3.60 | 3.60 | 3.60 | 3.60 | 3.60 | 3.60 | 3.60 | 3.60 | 3.60 |
| Asp | 3.16 | 3.16 | 3.16 | 3.16 | 3.16 | 3.16 | 3.16 | 3.16 | 3.16 | 3.16 |
| Cys-Cys | 0.50 | 0.50 | 0.50 | 0.50 | 0.50 | 0.50 | 0.50 | 0.50 | 0.50 | 0.50 |
| Gln | 9.16 | 12.76 | 11.64 | 13.70 | 16.22 | 10.35 | 11.15 | 11.50 | 9.94 | 12.74 |
| Glu | 9.16 | 9.16 | 9.16 | 9.16 | 9.16 | 9.16 | 9.16 | 9.16 | 9.16 | 9.16 |
| Gly | 1.62 | 1.62 | 1.62 | 1.62 | 1.62 | 1.62 | 1.62 | 1.62 | 1.62 | 1.62 |
| Pro | 9.37 | 9.37 | 9.37 | 9.37 | 9.37 | 9.37 | 9.37 | 9.37 | 9.37 | 9.37 |
| Ser | 5.06 | 5.06 | 5.06 | 5.06 | 5.06 | 5.06 | 5.06 | 5.06 | 5.06 | 5.06 |
| Tyr | 4.85 | 4.85 | 4.85 | 4.85 | 4.85 | 4.85 | 4.85 | 4.85 | 4.85 | 4.85 |
| AA-Total | 93.82 | 94.87 | 91.85 | 90.22 | 92.06 | 92.58 | 91.31 | 92.35 | 93.51 | 91.67 |
| Starch | 6.18 | 5.13 | 8.15 | 9.78 | 7.94 | 7.42 | 8.69 | 7.65 | 6.49 | 8.33 |
| Total | 100.00 | 100.00 | 100.00 | 100.00 | 100.00 | 100.00 | 100.00 | 100.00 | 100.00 | 100.00 |

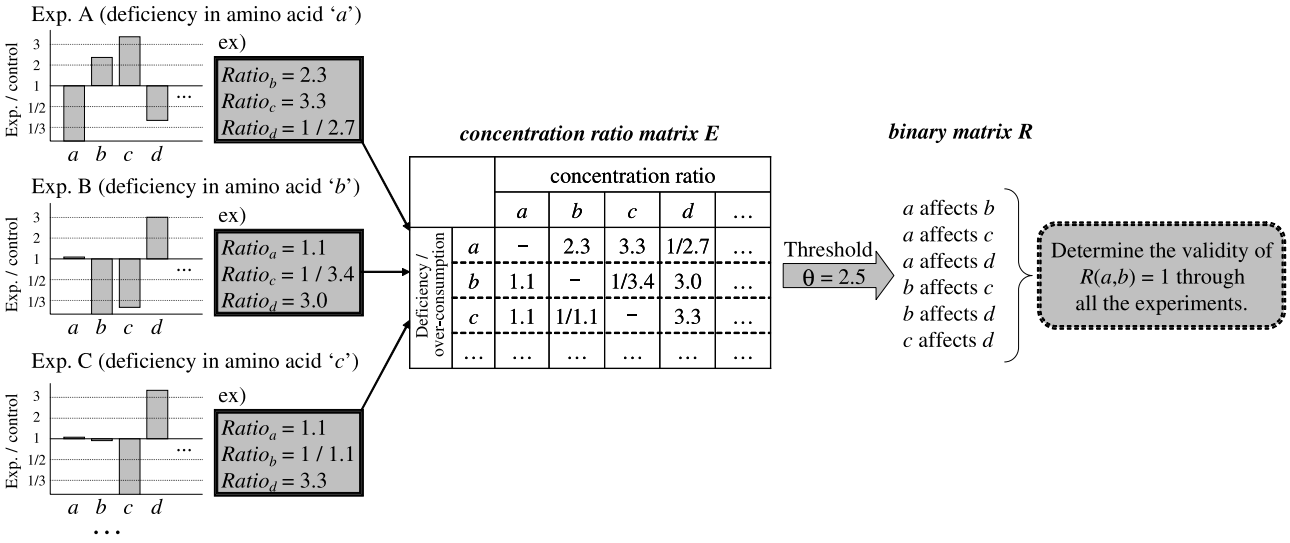


**Fig. 1.** Process of threshold-test analysis method

was filtrated with Ultrafree-MC filter (Cat. No. UFC3LGC00, Millipore), and the amino acid concentrations were measured by an automatic amino acid analyzer (L-8800; Hitachi, Tokyo, Japan).

*Inferring methods*

In this study, we are to use threshold-test analysis and the multi-level digraph analysis methods to infer amino acid networks. Using graphic approach or diagraph method to study biology-related can make the problem more intuitive, facilitating illustration and stimulating imagination so as to help reveal the essence of the problem concerned. Graphic approach has been successfully used to study enzyme-catalyzed system (Chou, 1981, 1989; Chou and Liu, 1981; Kuzmic et al., 1992; Lin and Neet, 1990), protein folding kinetics (Chou, 1990), HIV reverse transcriptase inhibition mechanisms (Althaus et al., 1993a, b, c; Chou et al., 1994), and analysis of base frequencies in the anti-sense strands of human protein coding sequences (Zhang and Chou, 1996). Recently, the images of cellular automata were used to investigate HBV virus gene missense mutation (Xiao et al., 2005a), HBV viral infections (Xiao et al., 2006b), represent biological sequences (Xiao et al., 2005b), predict protein subcellular location (Xiao et al., 2006a), and analyze the fingerprint of SARS coronavirus (Wang et al., 2005).

Our strategy for the inference of interrelated amino acid networks can be summarized as follow: (1) Given data of fold-change in concentration of deficiency or over-consumption in one essential amino acid under the stationary state, the threshold-test analysis method is applied to infer binary relationships between target amino acids. (2) The multi-level digraph analysis method infers consistent minimal binary relationships starting from many binary relationships derived from the threshold-test analysis method.

Threshold-test analysis method

A threshold-test analysis method treats the data representing the binary relations of change in the concentration of amino acids. These relations describe the effects of one amino acid on the concentration of the other amino acids and are mainly provided by the changes in the state of amino acid concentrations (Fig. 1). Upon setting an arbitrary threshold value of concentration ratio, one can extract binary relations between two amino acids directly by estimation of the relative change in concentration ratios ($\theta_F$) or by the statistical probability of change in average concentrations ($\theta_P$) from deficiency or over-consumption in one essential amino acid experimental data. The following method is explained using the concentration ratios ($\theta_F$) as an example. A set of amino acids is defined as $S = \{a, b, c, \ldots\}$. We assume here experiments are those of deficiency or over-consumption of one essential amino acid, and that the measurements of concentrations of many amino acids are performed simultaneously. The change in concentration of the amino acids resulting from the deficiency or over-consumption of one target amino acid relative to its concentration under normal conditions (control of amino acids) is examined and recorded. This change may be recorded as an increase, decrease, or no change. An concentration ratio matrix, E, is created from a set of deficiency in one amino acid (or over-consumption) experiments, in which each matrix element represents the real-valued ratio of amino acid concentration. For instance, the value of matrix element $E(a, b)$ indicates the relative change (the concentration ratio) in concentration of amino acid '$b$' in comparison to its concentration under control conditions caused by the deficiency (or over-consumption) in amino acid '$a$'. Thus the matrix E is defined as $E = \{(a, b), \ldots\}$. The inference procedures of this network model are as follows: (0) Obtain the concentration ratio matrix E using several sets of the amino acid concentrations resulting from deficiency or over-consumption of one essential amino acid. (1) Using the concentration ratio matrix E, we determine whether a given amino acid affects another given amino acid. For example, if, following the deficiency of amino acid '$a$', the ratio of amino acid '$b$' becomes higher than a given threshold value (specifically, more than $\theta_F$-times higher), or becomes lower than a given threshold value (specifically, less than $1/\theta_F$-times lower) we say that amino acid '$a$' affects amino acid '$b$' directly or indirectly, and the value of element ($a$, $b$) in the binary matrix $R$ is set to 1; $R(a, b) = 1$. (2) It should be noted that the condition amino acid '$a$' affects amino acid '$b$', that is $R(a, b)$ takes the value 1, means both "$a$ change in concentration-value of '$a$' leads to a change in that of '$b$'" and also "no change in the concentration-value of '$b$' leads to no change in that of '$a$'". Thus the probability of $R(a, b)$ takes the value 1, or more generally the probability that the value $R(i, j)$ takes the value 1, $P(R(i, j) = 1)$ (where $i, j = 1, 2, \ldots, n$ in which $n$ is the total number of target amino acid) is examined through all the experiments of deficiency or over-consumption of one essential amino acid. An arbitrary second threshold value for probability is set, $\rho$, and experimental events with $P(R(i, j) = 1) > \rho$ are extracted statistically.

Multi-level digraph analysis method

A multi-level digraph analysis method infers amino acid networks by using a set of binary relations between amino acid (e.g. amino acid '$a$' affects

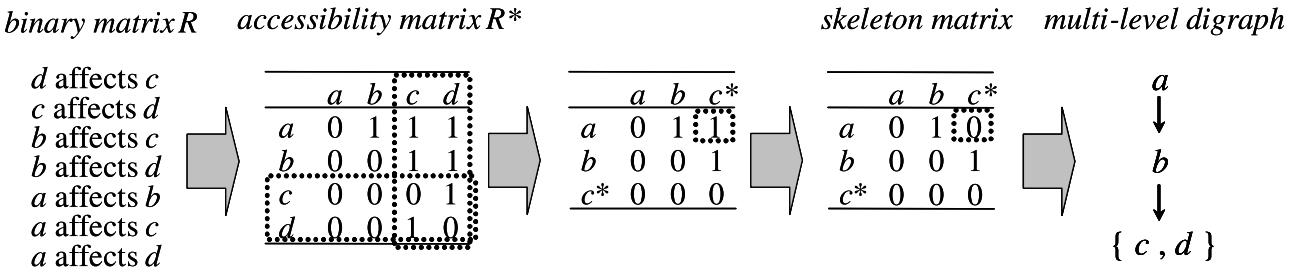


**Fig. 2.** Process of the multi-level digraph analysis method

amino acid '*b*') (Maki et al., 2001, 2004). A systematical analysis of the binary relations between pairs of amino acids enables us to reconstruct a possible minimum architecture of the amino acid network that is consistent with all of the data. In Fig. 2, the accessibility matrix $R^*$ is derived directly from the binary relation $R$. In the accessibility matrix $R^*$, if there exists the relation that amino acid '*a*' and '*b*' affect each other, that is that $R^*(a, b) = R^*(b, a) = 1$, we cannot decide which amino acid is located at the upper stream. We therefore introduce an "equivalence set", which makes a single set of the group of amino acids affect each other, and this group is deemed to be a single amino acid. In order to partition amino acids into equivalence sets, we use the accessibility matrix $R^*$. This matrix is a relative transitive closure of the binary relation matrix, $R$,

$$R^* = \bigcup_{n=0}^{x} R^n \begin{cases} R^0(i,j) = \begin{cases} 1 : i = j \\ 0 : i \neq j \end{cases} \\ R^{n+1} = \min(1, \sum_k R^n(i,j) \cdot R(k,j)) \end{cases} \quad (1)$$

where the matrix entry $R^*(a, b)$ indicates whether amino acid '*a*' finally affects amino acid '*b*' or not. The multi-level digraph analysis model is implemented on the basis of this accessibility matrix $R^*$. Figure 2 shows the procedure for drawing a multi-level digraph. For the accessibility matrix $R^*$ in the figure, since '*c*' and '*d*' can be regarded as an equivalence set, we can combine them as '$c^*$'. In this manner, we can draw up equivalence sets in a semi-ordered (topologically sorted) accessibility matrix. A semi-ordered accessibility matrix between equivalence sets includes indirect amino acid relations. In order to remove them and to make a skeleton matrix, we process the semi-ordered matrix as follows: The value of line $i$ and column $j$ in a semi-ordered matrix A and skeleton matrix S are represented as $A(i,j)$ and $S(i,j)$, respectively. If $A(i,j) = 1$, $S(i,k)(k = 1, \ldots, n)$ is set to $\max\{A(i,j) - A(j,k), 0\}$. Thus, all indirect effects are removed from the semi-ordered matrix. In Fig. 2, the relation between amino acid '*a*' and '$c^*$' are removed, we thus can construct the skeleton matrix S. Finally we draw lines between nodes based on the value

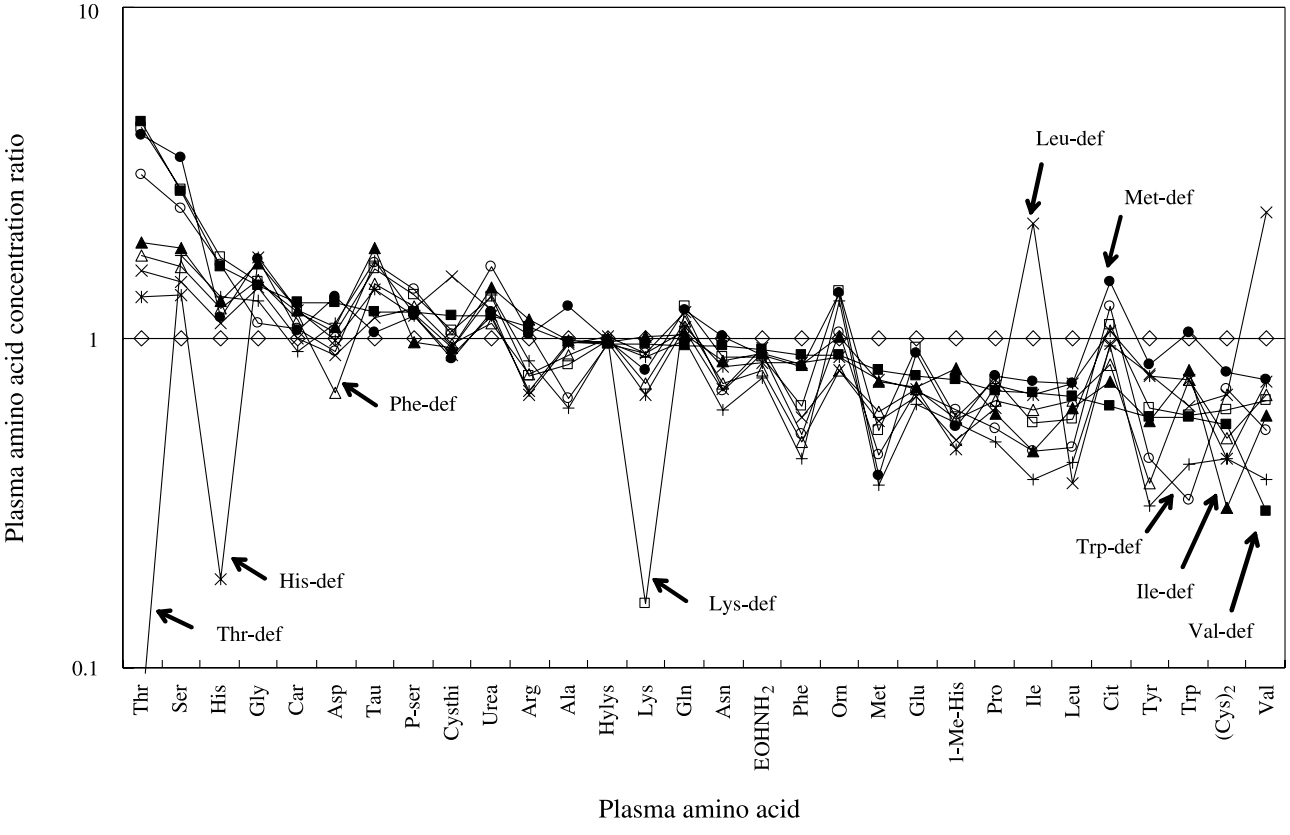


**Fig. 3.** Plasma amino acid concentration ratio. The concentration of plasma amino acid by amino acid minus-one diet is shown as the ratio to that of control diet

of each element in the skeleton matrix. In Fig. 2, the amino acids with parentheses indicate an equivalence set of amino acids.

## Results

### *Constructing binary interaction matrix for plasma amino acids*

The sample plasma was obtained from the amino acid minus-one diet fed rats, whose plasma concentration of the deficient amino acid is less than half of that of the control diet fed rats. Deficiency in one essential amino acid triggers the change in concentrations of all the other amino acids in plasma as shown in Fig. 3. This change is converted to the directional relation from the deficient amino acids to all the other amino acids by the described method. Two different values were adopted to set the threshold. One is the fold-change value ($\theta_F$-value). Larger $\theta_F$-value means the severer filtering condition. The other value is the *p*-value (level of significance) for the average difference ($\theta_P$-value). Each experimental and control groups consist of 6 samples, and for all the amino acids measured, the *p*-value, level of significance, for the average difference between the experimental group and the control group was calculated using Dunnet's multiple comparison method. In this case, smaller $\theta_P$-value means the severer filtering condition.

### *Network structure estimated by the multi-level digraph method*

From the binary interaction matrix, multi-scale digraph was drawn (Fig. 4). In the analysis using fold-change value as the threshold, the number of amino acids (nodes) composing the network decreases as the filtering threshold becomes severer. In the analysis using the *p*-value (level of significance), the number of nodes does not change drastically as the threshold changes.

In either analysis, some amino acids formed an equivalence group, in which the interactions (links) form a loop and the direction of the effect on one another cannot be

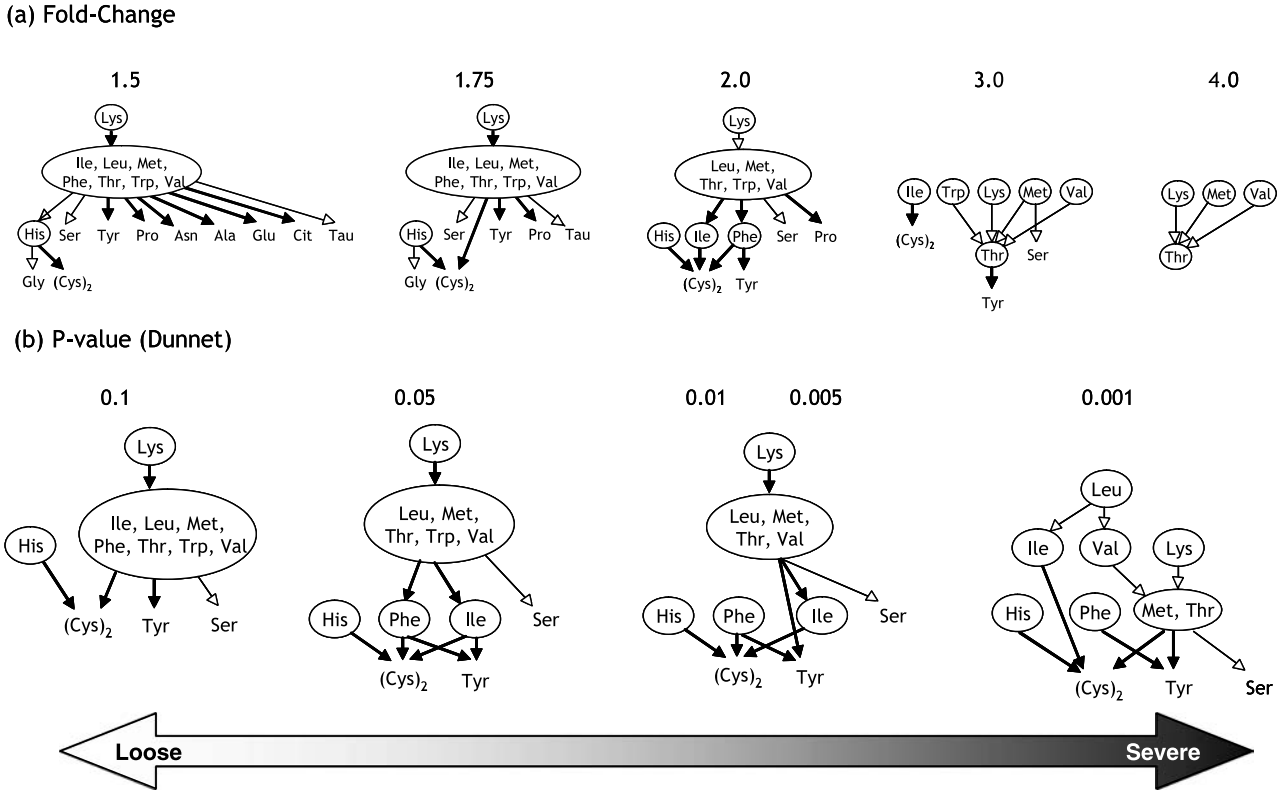


**Fig. 4.** Network structure estimated by threshold-test analysis and multi-level digraph analysis methods. Network structure of plasma amino acids is estimated using threshold-test analysis and multi-level digraph analysis methods. The amino acids whose minus-one diet experiments were performed are indicated in circles. The change in plasma amino acid concentration was converted to binary relational values, in the manner described in the results. The threshold to determine the binary value is set using **a** fold-change ($\theta_F$-value) and **b** *p*-value ($\theta_P$-value). For both cases, the figures to the right uses severer threshold in determining the binary values. Lines with black arrowheads indicate the positive effects and the lines with white arrowheads indicate the negative effects

decided. When the filtering condition becomes severer, the link forming the loop is disappeared and the equivalence group disperses into the smaller groups or individual amino acids. In the case using fold-change value, the equivalence group disperses at the threshold of 3.0, and 3-level digraph with 9 amino acids is drawn. In the case using $p$-value, the equivalence group does not completely disappear and at the threshold $p = 0.001$, which is the severest condition inspected, 4-level digraph with 11 amino acids is drawn. Since we should like to infer network model with as many nodes and links as possible, we decided to use $p$-value for the threshold for the further analysis.

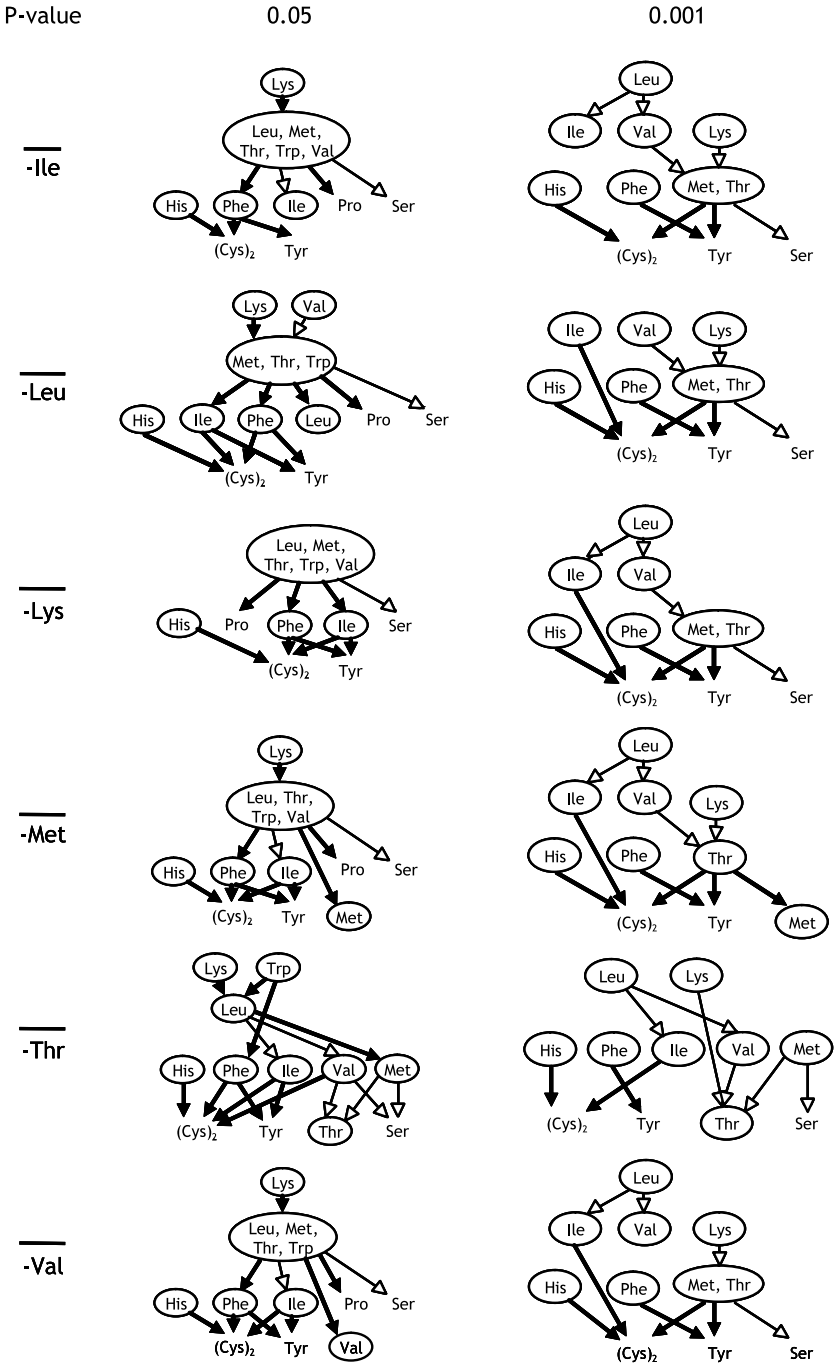


**Fig. 5.** Network estimated from partial data. The minus-one dataset left out from the analysis is indicated in the left column. Each horizontal row uses the same partial dataset for analysis. The figures to the right uses severer threshold in determining the binary values. Lines with black arrowheads indicate the positive effects and the lines with white arrowheads indicate the negative effects

*Effect of each amino acid on the network structure*

The same analysis was carried out using the partial dataset. By excluding one amino acid minus-one dataset, we can estimate the network structure without considering the effect of the excluded amino acid. The results are shown in Fig. 5. At the threshold $p = 0.05$, the removal of threonine minus-one dataset changed the network structure drastically. The equivalence group disappears and the interactions between the amino acids which belonged to the group are alternatively revealed. This indicates that the relation responsible for holding the equivalence group together was the effect of threonine on the other amino acids, leucine, methionine, tryptophan and valine, in the group. At the threshold $p = 0.001$, the only amino acids forming the equivalence group are threonine and methionine. By excluding threonine minus-one dataset, the effects of methionine on other amino acids are revealed, and by excluding methionine minus-one dataset, the effects of threonine are revealed. Integrating the information obtained from the analysis of partial dataset, the estimated network structure is further refined to the model shown in Fig. 6. Threonine directly interacts with the most number of amino acids, and lysine is located at the top control level in all the other amino acids. Threonine and methionine is interrelated each other, which forms a feedback loop.

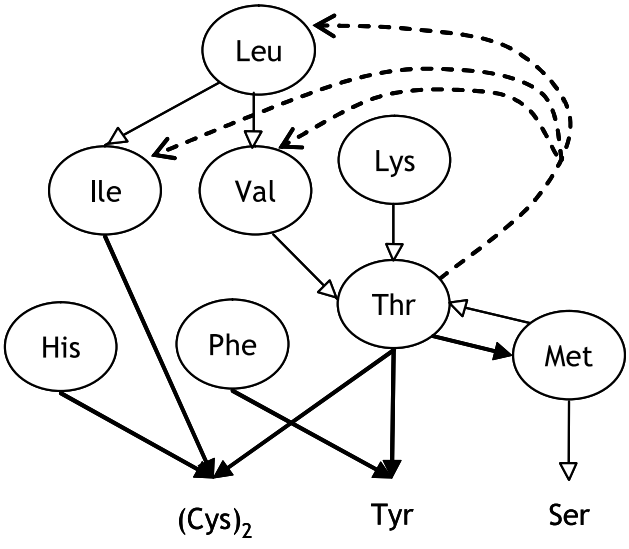


**Fig. 6.** Refined network structure of plasma amino acids. The network structure estimated in Fig. 4. is refined using results of the partial dataset analysis in Fig. 5. Lines with black arrowheads indicate the positive effects and the lines with white arrowheads indicate the negative effects. Dashed lines indicate the relationship extracted under loose threshold value

## Discussion

Using the data obtained under the essential amino acid minus-one condition, we have first estimated the coarse network structure of the plasma amino acids. The minus-one condition lowers the plasma concentration of the deficient amino acid to less than half, and this condition was maintained for a fairly long period. This drop in the concentration and the consequent changes in other amino acid concentrations are theoretically equivalent to the single gene disruption experiments in which the expression of the disrupted gene drops to nearly zero and the expression of the other genes are altered. In these experiments the genes whose expression levels were altered are suggested to be directly or indirectly regulated by the disrupted genes. Similarly, the amino acids whose plasma concentration changed under minus-one condition are suggested to be directly or indirectly regulated by the deficient amino acid. Combining the essential amino acid minus-one datasets, we were able to draw a coarse network model which can explain the change in the concentration of the plasma amino acids in our experiments.

*Role of lysine and threonine in the network*

In the estimated plasma amino acid network structure, lysine is located at the top control level, which affects most of the amino acids, but is not influenced by any amino acids. This indicates the biological essentiality of lysine in an organism. Lysine deficiency is the strongest signal and the wide range of amino acid metabolism has to be modulated to mitigate the damage. Threonine interacts directly with the most number of the amino acids, acting as a hub in the network. This suggests the possible role of plasma threonine as a messenger which spreads the information of any essential amino acid deficiency to the whole body. When rats are fed minus-one diet, they will respond by changing their metabolic flow, to save and recycle the limited amino acid (Kimball, 2002) and compensate for the shortage by making use of internal amino acid pool, such as skeletal muscle (Kadowaki and Kanazawa, 2003). In this regulation of metabolic rate, threonine might play an important role. The concentration of threonine rises in any amino acid minus-one condition, except for threonine minus-one. Thus it is highly possible that threonine may be used to regulate the pathway which will be needed in any essential amino acid shortages.

*Threonine-methionine loop*

As shown in Fig. 6, we can speculate that threonine gives positive influence to methionine, and methionine gives

negative influence to threonine. These positive and negative interactions make up a loop which causes the temporal oscillatory behavior of the threonine-methionine concentration. This kind of oscillation can play a role in a trigger switch in a biological system. One of the mutual relationships that link threonine and methionine is the common catabolic pathway downstream of 2-oxobutanoate. Threonine is deaminated to form 2-oxobutanoate (Kapke and Davis, 1976; Scarselli et al., 2003), and methionine forms 2-oxobutanoate via L-homocysteine and cystathionine (Stabler et al., 1993). This can partly explain the positive effect of threonine on methionine. When the concentration of plasma threonine decreases, the concentrations of 2-oxobutanoate may also decrease and the methionine catabolism may be stimulated. Cystathionine beta-synthase usually catalyzes the reaction of replacing beta-OH of serine by homocysteine, however, it is reported that threonine can be substituted for serine in this reaction forming 3-methylcystathionine (Borcsok and Abeles, 1982). Cystathionine beta-synthase is a key enzyme in methionine metabolism which directs the metabolite flux towards catabolic trans-sulfuration pathway rather than methionine recycling salvage pathway (Banerjee and Zou, 2005). The fact that threonine can be a counter substrate for this enzyme indicates the possibility of threonine having direct regulatory effect on methionine metabolism. Another possible link between threonine and methionine is vitamin B12. There are two enzymes which require vitamin B12, L-methylmalonyl-CoA mutase and methionine synthase. L-methylmalonyl-CoA mutase catalyzes the conversion of L-methylmalonyl-CoA to succinyl-CoA. L-methylmalonyl-CoA is one of the metabolites of threonine. Methionine synthase catalyzes the conversion of 5-$CH_3$-tetrahydrofolate and homocysteine to tetrahydrofolate and methionine, respectively (Allen et al., 1993; Watanabe and Nakano, 1999). This may be a clue which explains the negative effect of methionine to threonine.

The model reported in this study is constructed using the static plasma amino acid data obtained in a condition where plasma amino acids concentration had been equilibrated by the minus-one condition. It is a snapshot or a cross section, taken under this particular minus-one condition, of the dynamic plasma amino acid network. It is constructed without any prior topological information of the amino acid metabolic pathway, however, it is notable that some relations in the model, such as the direct relation of phenylalanine to tyrosine, can be explained by the pathway map. By comparing and integrating snapshots taken under various conditions, we can refine and validate the estimated network structure of the plasma amino acid.

## References


Allen RH, Stabler SP, Savage DG, Lindenbaum J (1993) Metabolic abnormalities in cobalamin (vitamin B12) and folate deficiency. Faseb J 7: 1344–1353

Althaus IW, Chou JJ, Gonzales AJ, Deibel MR, Chou KC, Kezdy FJ, Romero DL, Aristoff PA, Tarpley WG, Reusser F (1993a) Steady-state kinetic studies with the non-nucleoside HIV-1 reverse transcriptase inhibitor U-87201E. J Biol Chem 268: 6119–6124

Althaus IW, Chou JJ, Gonzales AJ, Deibel MR, Chou KC, Kezdy FJ, Romero DL, Palmer JR, Thomas RC, Aristoff PA, et al. (1993b) Kinetic studies with the non-nucleoside HIV-1 reverse transcriptase inhibitor U-88204E. Biochemistry 32: 6548–6554

Althaus IW, Gonzales AJ, Chou JJ, Romero DL, Deibel MR, Chou KC, Kezdy FJ, Resnick L, Busso ME, So AG, et al. (1993c) The quinoline U-78036 is a potent inhibitor of HIV-1 reverse transcriptase. J Biol Chem 268: 14875–14880

Banerjee R, Zou CG (2005) Redox regulation and reaction mechanism of human cystathionine-beta-synthase: a PLP-dependent hemesensor protein. Arch Biochem Biophys 433: 144–156

Borcsok E, Abeles RH (1982) Mechanism of action of cystathionine synthase. Arch Biochem Biophys 213: 695–707

Chou KC (1981) Two new schematic rules for rate laws of enzyme-catalysed reactions. J Theor Biol 89: 581–592

Chou KC (1989) Graphic rules in steady and non-steady state enzyme kinetics. J Biol Chem 264: 12074–12079

Chou KC (1990) Applications of graph theory to enzyme kinetics and protein folding kinetics. Steady and non-steady-state systems. Biophys Chem 35: 1–24

Chou KC, Liu WM (1981) Graphical rules for non-steady state enzyme kinetics. J Theor Biol 91: 637–654

Chou KC, Kezdy FJ, Reusser F (1994) Kinetics of processive nucleic acid polymerases and nucleases. Anal Biochem 221: 217

Chou KC, Cai YD, Zhong WZ (2006) Predicting networking couples for metabolic pathways of Arabidopsis. EXCLI J 5: 55–65

Felig P (1975) Amino acid metabolism in man. Annu Rev Biochem 44: 933–955

Ferenci P, Wewalka F (1978) Plasma amino acids in hepatic encephalopathy. J Neural Transm [Suppl] 14: 87–94

Holm E, Sedlaczek O, Grips E (1999) Amino acid metabolism in liver disease. Curr Opin Clin Nutr Metab Care 2: 47–53

Hong SY, Yang DH, Chang SK (1998) The relationship between plasma homocysteine and amino acid concentrations in patients with end-stage renal disease. J Ren Nutr 8: 34–39

Jimenez Jimenez FJ, Ortiz Leyba C, Morales Menedez S, Barros Perez M, Munoz Garcia J (1991) Prospective study on the efficacy of branched-chain amino acids in septic patients. JPEN 15: 252–261

Kadowaki M, Kanazawa T (2003) Amino acids as regulators of proteolysis. J Nutr 133: 2052S–2056S

Kapke G, Davis L (1976) Stereochemistry of the reaction of sheep liver threonine dehydratase. A nuclear magnetic resonance and optical rotatory dispersion study of its reaction pathway and products. Biochemistry 15: 3745–3749

Kimball SR (2002) Regulation of global and specific mRNA translation by amino acids. J Nutr 132: 883–886

Kuzmic P, Ng KY, Heath TD (1992) Mixtures of tight-binding enzyme inhibitors. Kinetic analysis by a recursive rate equation. Anal Biochem 200: 68–73

Lin SX, Neet KE (1990) Demonstration of a slow conformational change in liver glucokinase by fluorescence spectroscopy. J Biol Chem 265: 9670–9675

Maki Y, Takahashi Y, Arikawa Y, Watanabe S, Aoshima K, Eguchi Y, Ueda T, Aburatani S, Kuhara S, Okamoto M (2004) An integrated

comprehensive workbench for inferring genetic networks: voyagene. J Bioinform Comput Biol 2: 533–550

Maki Y, Tominaga D, Okamoto M, Watanabe S, Eguchi Y (2001) Development of a system for the inference of large scale genetic networks. Pac Symp Biocomput 6: 446–458

Nicholson JK, Lindon JC, Holmes E (1999) 'Metabonomics': understanding the metabolic responses of living systems to pathophysiological stimuli via multivariate statistical analysis of biological NMR spectroscopic data. Xenobiotica 29: 1181–1189

Noguchi Y, Zhang QW, Sugimoto T, Furuhata Y, Sakai R, Mori M, Takahashi M, Kimura T (2006) Network analysis of plasma and tissue amino acids and the generation of an amino index for potential diagnostic use. Am J Clin Nutr 83: 513S–519S

Scarselli M, Padula MG, Bernini A, Spiga O, Ciutti A, Leoncini R, Vannoni D, Marinello E, Niccolai N (2003) Structure and function correlations between the rat liver threonine deaminase and aminotransferases. Biochim Biophys Acta 1645: 40–48

Soeters PB, Fischer JE (1976) Insulin, glucagon, aminoacid imbalance, and hepatic encephalopathy. Lancet 2: 880–882

Stabler SP, Lindenbaum J, Savage DG, Allen RH (1993) Elevation of serum cystathionine levels in patients with cobalamin and folate deficiency. Blood 81: 3404–3413

Tudor I, Tanase-Mogos I, Tanasie E, Badescu E, Rascanu M (1976) A study of aminoacidemia and aminoaciduria in epileptic children. Neurol Psychiatr (Bucur) 14: 277–282

Wang M, Yao JS, Huang ZD, Xu ZJ, Liu GP, Zhao HY, Wang XY, Yang J, Zhu YS, Chou KC (2005) A new nucleotide-composition based fingerprint of SARS-CoV with visualization analysis. Med Chem 1: 39–47

Watanabe A, Higashi T, Sakata T, Nagashima H (1984) Serum amino acid levels in patients with hepatocellular carcinoma. Cancer 54: 1875–1882

Watanabe A, Takei N, Hayashi S, Nagashima H (1983) Serum neutral amino acid concentrations in cirrhotic patients with impaired carbohydrate metabolism. Acta Med Okayama 37: 381–384

Watanabe F, Nakano Y (1999) [Vitamin B12]. Nippon Rinsho 57: 2205–2210

Xiao X, Shao S, Ding Y, Huang Z, Chen X, Chou KC (2005a) An application of gene comparative image for predicting the effect on replication ratio by HBV virus gene missense mutation. J Theor Biol 235: 555–565

Xiao X, Shao S, Ding Y, Huang Z, Chen X, Chou KC (2005b) Using cellular automata to generate image representation for biological sequences. Amino Acids 28: 29–35

Xiao X, Shao S, Ding Y, Huang Z, Chou KC (2006a) Using cellular automata images and pseudo amino acid composition to predict protein subcellular location. Amino Acids 30: 49–54

Xiao X, Shao SH, Chou KC (2006b) A probability cellular automaton model for hepatitis B viral infections. Biochem Biophys Res Commun 342: 605–610

Yeang CH, Mak HC, McCuine S, Workman C, Jaakkola T, Ideker T (2005) Validation and refinement of gene-regulatory pathways on a network of physical interactions. Genome Biol 6: R62

Zhang CT, Chou KC (1996) An analysis of base frequencies in the antisense strands corresponding to the 180 human protein coding sequences. Amino Acids 10: 253–262

**Authors' address:** Nahoko Shikata, Graduate School of Systems Life Sciences, Kyushu University, 6-10-1 Hakozaki, Higashi-ku, Fukuoka 812-8581, Japan,
Fax: +81-44-244-9617, E-mail: shikata@brs.kyushu-u.ac.jp